UDC 544.723; 669.788

INFLUENCE OF THE HYDROGEN SATURATION TEMPERATURE ON THE STRUCTURE OF MELT-SPUN $Ti_{30}Zr_{45}Ni_{25}$ ALLOY

O.Ye. Dmytrenko, I.V. Kolodiy
National Science Center "Kharkov Institute of Physics and Technology", Kharkov, Ukraine
E-mail: dmitrenko@kipt.kharkov.ua

The influence of hydrogen saturation temperature on the structure and phase composition of the melt-spun $Ti_{30}Zr_{45}Ni_{25}$ alloys, heat-treated in hydrogen atmosphere at different temperatures (400, 450, 500 °C) for 4 hours, was studied. Using X-ray diffraction analysis it was found that hydrides, formed during the hydrogenation process, were based on the Laves phase L-TiZrNi and $(Ti, Zr)_2Ni$, α-(Ti, Zr) phases. Structural models of these phases were constructed and a model for filling these phases with hydrogen was presented. Electron microscopic study showed that the surface of the samples had no significant changes during the hydrogenation process. Also, it was established the influence of the hydrogenation temperature on the concentration of oxygen and nitrogen gas impurities in the samples.

INTRODUCTION

Ti-Zr-Ni alloys have received much attention in recent years due to their ability to absorb fairly high amount of hydrogen. Moreover, the alloys desorb most of the absorbed hydrogen in the moderate temperature range of 400…500 °C without phase transformation. The hydrogen uptake depends on the structure state of material. The microstructure and phase content of the Ti-Zr-Ni alloys, presenting Laves phases, amorphous phases or quasicrystals, is strongly dependent on the chemical composition and way of production. It was found that amount of absorbed hydrogen by melt-spun $Ti_{30}Zr_{45}Ni_{25}$ alloy was about 1.7 wt.% [1]. However, the maximum absorbed hydrogen uptake for Ti-Zr-Ni alloys was up to 2.3 wt.% [2–4]. The purpose of this paper is to establish the correlation between microstructure, phase composition and hydrogen storage capacity of as-cast and melt-spun Ti-Zr-Ni alloys.

EXPERIMENTAL

Basic $Ti_{30}Zr_{45}Ni_{25}$ alloy was prepared by vacuum arc-melting of high-purity components in the pure Ar atmosphere (Ti – 99.98%, Zr – 99.98%, Ni – 99.98%). The as-cast ingot was then melt-spun under pure argon using a copper wheel with a surface speed of 30 m/s. Typical thickness of melt-spun $Ti_{30}Zr_{45}Ni_{25}$ ribbons was about 40…60 μm. The hydrogenation was performed in the gas phase. The H_2 pressure was 0.5 atm within 4 hours under 3 different temperatures of 400, 450, 500 °C [5]. The following samples were taken for this study:

1. $Ti_{30}Zr_{45}Ni_{25}$ arc-vacuum melted ingot;
2. $Ti_{30}Zr_{45}Ni_{25}$ melt-spun alloy;
3. $Ti_{30}Zr_{45}Ni_{25}$ melt-spun alloy + H_2 at T = 400 ºC;
4. $Ti_{30}Zr_{45}Ni_{25}$ melt-spun alloy + H_2 at T = 450 ºC;
5. $Ti_{30}Zr_{45}Ni_{25}$ melt-spun alloy + H_2 at T = 500 ºC.

A DRON-4 diffractometer with Cu-Kα-radiation was used to study crystal structure and phase composition of samples by X-ray diffraction (XRD). Phase composition and structural parameters of phases were determined by Rietveld refinement (Powder Cell, Maud). The hydrogen amount in the hydrides (stoichiometric coefficients in the chemical formula) was determined by approximating the corresponding literature values of the relative change in the unit cell volume [6–8].

SEM and EDX analyses were performed using QUANTA 200 3D microscope and Pegasus 2000 probe. The oxygen and nitrogen content was measured by LECO TC-600 gas analyzer. The accuracy of O_2 and N measurements was 0.05 ppm. The hydrogen desorption from the alloys was studied by MX7203 mass-spectrometer in the temperature range of 0…800 °C [9].

RESULTS AND DISCUSSION

Diffraction patterns of the investigated samples are shown in Fig. 1, the results of XRD analysis are presented in Tabl. 1. As-cast ingot (sample 1) presents 2 phases: hexagonal Laves phase L-TiZrNi (C14 type, $MgZn_2$ structure type) [10] and α-(Ti, Zr) phase (solid solution, based on Ti and Zr). The weight fractions of present phases are equal approximately 98 wt.% of L-TiZrNi and 2 wt.% of α-(Ti, Zr). Lattice parameters of Laves phase are: a = 5.2250 Å; c = 8.5509 Å, unit cell volume equal to V = 202.17 Å^3. It is impossible to determine lattice parameters of α-(Ti, Zr) solid solution, due to the small amount in the sample there is only one diffraction line of this phase on the diffraction pattern.

XRD analysis of the melt-spun alloy (see sample 2, Fig. 1,a) shows that specimen has two-phase structure of the Laves phase and $(Ti, Zr)_2Ni$ phase (Ti_2Ni-type with FCC structure, space group is Fd3m [11]). The main phase is L-TiZrNi Laves phase with lattice parameters a = 5.2294 Å; c = 8.5621 Å, the unit cell volume is V = 202.78 Å^3. As can be seen, the lattice parameters (and the unit cell volume) of the Laves phase after melt-spinning are greater than the corresponding values for the as-cast sample. Weight fraction of the L-TiZrNi phase in the sample is 86.2 wt.%. Besides, the sample contains a $(Ti, Zr)_2Ni$ phase (with lattice parameter a = 11.913 Å and unit cell volume V = 1690.69 Å^3). In this phase a part of the Ti atomic positions are replaced by Zr. According to the Vegard's rule, the relationship between Ti and Zr is determined ($X_{Ti} \approx 0.33$; $X_{Zr} \approx 0.66$). The weight fraction of $(Ti, Zr)_2Ni$ phase is 13.8 wt.%. Availability of $(Ti, Zr)_2Ni$ phase is caused by the presence of oxygen in metal matrix (~ 0.132 wt.%), which destabilizes the quasycrystalline i-phase and the Laves phase [12–14].

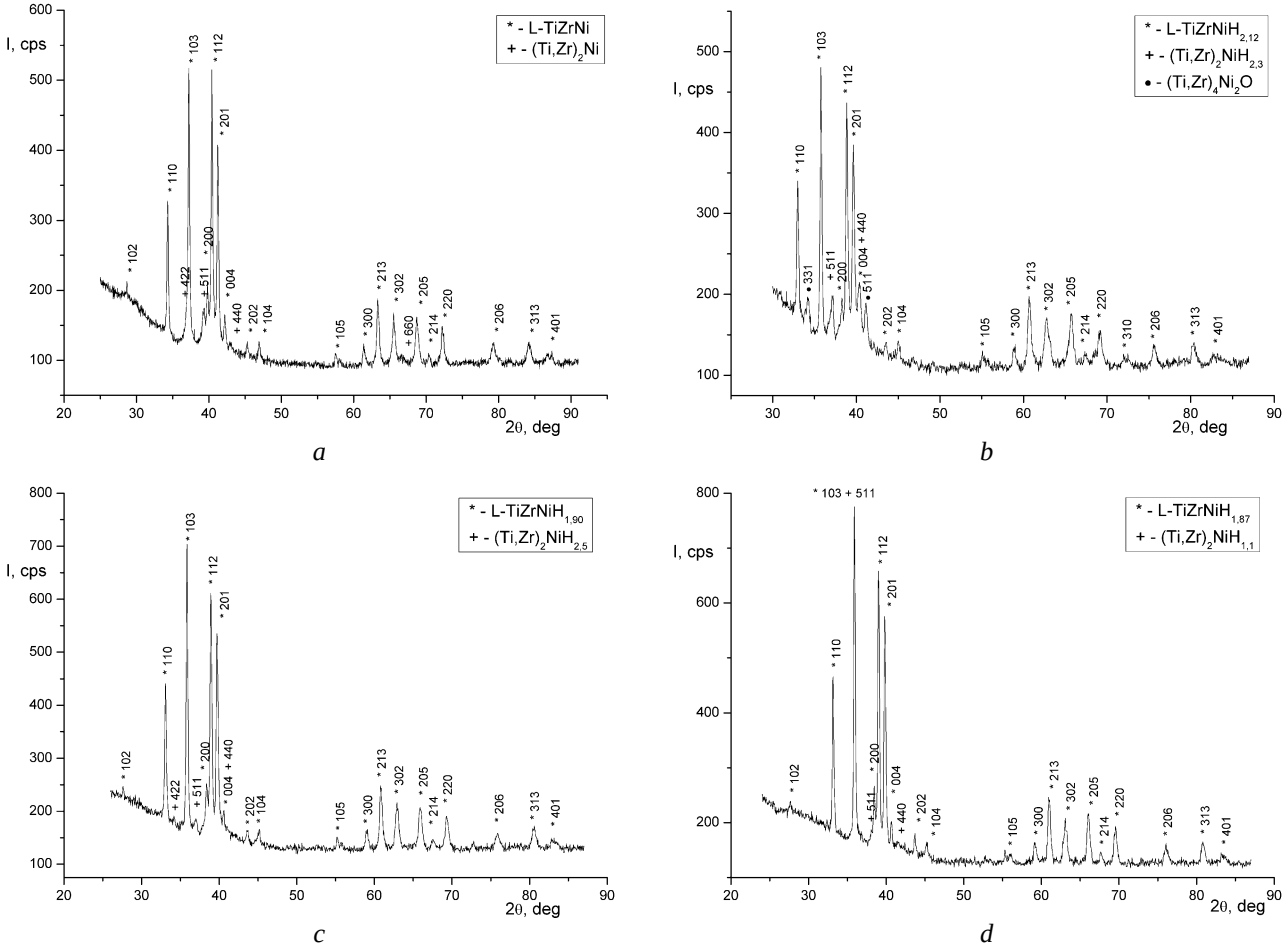

Fig. 1. XRD patterns of the samples: a – melt-spun $Ti_{30}Zr_{45}Ni_{25}$ alloy; b – melt-spun $Ti_{30}Zr_{45}Ni_{25}$ + H_2 at T = 400 ºC; c – melt-spun $Ti_{30}Zr_{45}Ni_{25}$ + H_2 at T = 450 ºC; d – melt-spun $Ti_{30}Zr_{45}Ni_{25}$ + H_2 at T = 500 ºC

Table 1

Results of the XRD analysis

No	Phase	Weight composition, %	Lattice parameters, Å	Unit cell volume V, Å^3	Relative change in the unit cell volume ΔV/V, %
1	L-TiZrNi	98	a = 5.2250, c = 8.5509	202.17	–
	α-(Ti,Zr)	2	–	–	–
2	L-TiZrNi	86.2	a = 5.2294, c = 8.5621	202.78	–
	$(Ti,Zr)_2Ni$	13.8	a = 11.913	1690.69	–
3	$L\text{-}TiZrNiH_{2.12}$	82.0	a = 5.4280, c = 8.9191	227.58	12.7
	$(Ti,Zr)_2NiH_{2.3}$	9.6	a = 12.586	1993.72	17.9
	$(Ti,Zr)_4Ni_2O$	8.4	a = 11.398	1480.76	–
4	$L\text{-}TiZrNiH_{1.90}$	97.9	a = 5.4160, c = 8.8938	225.93	11.4
	$(Ti,Zr)_2NiH_{2.5}$	2.1	a = 12.616	2008.01	18.8
5	$L\text{-}TiZrNiH_{1.87}$	96.3	a = 5.4040, c = 8.8927	224.90	10.9
	$(Ti,Zr)_2NiH_{1.1}$	3.7	a = 12.270	1847.28	9.3

After the hydrogenation of melt-spun alloy at T = 400 ºC it is revealed three phases in the sample (see Fig. 1,b). The main phase is $L\text{-}TiZrNiH_{2.12}$ hydride (weight fraction – 82.0 wt.%). Lattice parameters of the $L\text{-}TiZrNiH_{2.12}$ phase are: a = 5.4280 Å; c = 8.9191 Å, and unit cell volume equal V = 227.58 Å^3 (ΔV = 25.8 and $\Delta V/V$ = 12.7%). Besides the Laves phase hydride there is a $(Ti, Zr)_2NiH_{2.3}$ hydride with weight fraction 9.6 wt.% in the specimen. Lattice parameter of this phase is equal to a = 12.586 Å; unit cell volume V = 1993.72 Å^3 and $\Delta V/V$ = 17.9%. Also, the oxygen-containing phase $(Ti, Zr)_4Ni_2O$ [14] is revealed in the sample in amount of 8.4 wt.% (lattice parameter a = 11.398 Å, unit cell volume V = 1480.76 Å^3). Judging by the lattice parameter, this phase does not participate in the hydrogen storage process. Apparently the presence of oxygen blocks the hydrogen diffusion into the lattice.

After the hydrogenation of melt-spun alloy at T = 450 ºC (see Fig. 1,c) the main phase in the specimen is Laves phase hydride $L\text{-}TiZrNiH_{1.90}$ (weight fraction is 97.9 wt.%). Lattice parameters of the $L\text{-}TiZrNiH_{1.90}$

phase are equal: a = 5.4160 Å; c = 8.8938 Å, unit cell volume is V = 225.93 Å^3 (ΔV = 23.2, $\Delta V/V$ = 11.4%). Also, (Ti, Zr)$_2$NiH$_{2.5}$ hydride coexists in the sample (weight fraction – 2.1 wt.%, lattice parameter a = 12.616 Å; V = 2008.01 Å^3, ΔV = 317.32, and $\Delta V/V$ = 18.8%).

After the hydrogenation of melt-spun alloy at T = 500 ºC (see Fig. 1,d) two hydrides coexist in the sample: Laves phase hydride L-TiZrNiH$_{1.87}$ (weight fraction 96.3 wt.%, lattice parameters are a = 5.4040 Å; c = 8.8927 Å, unit cell volume equal to V = 224.90 Å^3) and (Ti, Zr)$_2$NiH$_{1.1}$ hydride (weight fraction 3.7%wt, lattice parameter a = 12.270 Å; V = 1847.28 Å^3). Relative change in the unit cell volume of the Laves phase is $\Delta V/V$ = 10.9%. Relative change in the unit cell volume of the (Ti, Zr)$_2$NiH$_{1.1}$ hydride is $\Delta V/V$ = 9.3%.

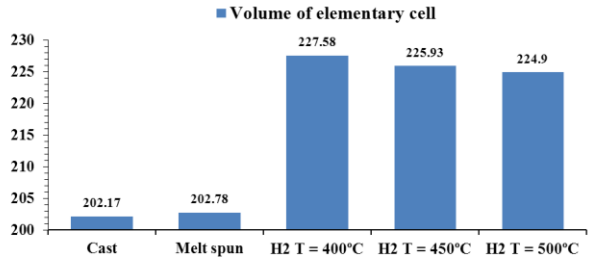

Fig. 2. Relative change in the unit cell volume of the Laves phase L-TiZrNiH$_x$ hydrides

Analysis of the obtained data shows, that relative change in the unit cell volume of the Laves phase (due to the hydrogen atoms implantation) has maximum value after the hydrogenation at T = 400 ºC and is equal to $\Delta V/V$ = 12.7% (Fig. 2). This value decreases with increasing the hydrogenation temperature. Therefore, it is obviously that the L-TiZrNi phase absorbs the maximum amount of hydrogen at 400 °C. A graph dependency of the relative change in the unit cell volume of L-TiZrNiH$_x$ and (Ti, Zr)$_2$NiH$_x$ phases on the hydrogen stoichiometric coefficient is shown on Fig. 3.

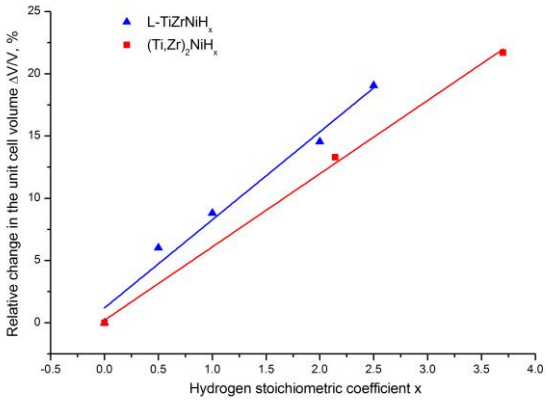

Fig. 3. Dependency of the relative change in the unit cell volume of L-TiZrNiH$_x$ and (Ti, Zr)$_2$NiH$_x$ phases on the hydrogen stoichiometric coefficient

On the basis of the published data [4] and conducted XRD studies the crystal structure models of the phases, presented in the samples, were built. Analysis of the L-TiZrNiH$_{2.12}$ structure model shows that its unit cell consists of 22.5 atoms (12 of them – metallic atoms, and 10.5 – hydrogen atoms). Wherein, hydrogen in this crystal structure does not completely occupy its positions. In the case of 100% hydrogen site occupancy it is theoretically possible to obtain structure L-TiZrNiH$_{12}$ H:M ratio 4:1 (hydrogen storage 5.73 wt.%). This theoretical structure should consist of 60 atoms, 48 of which are hydrogen. Crystal structure models of the L-TiZrNiH$_x$ phase with different hydrogen content are shown in Fig. 4,a.

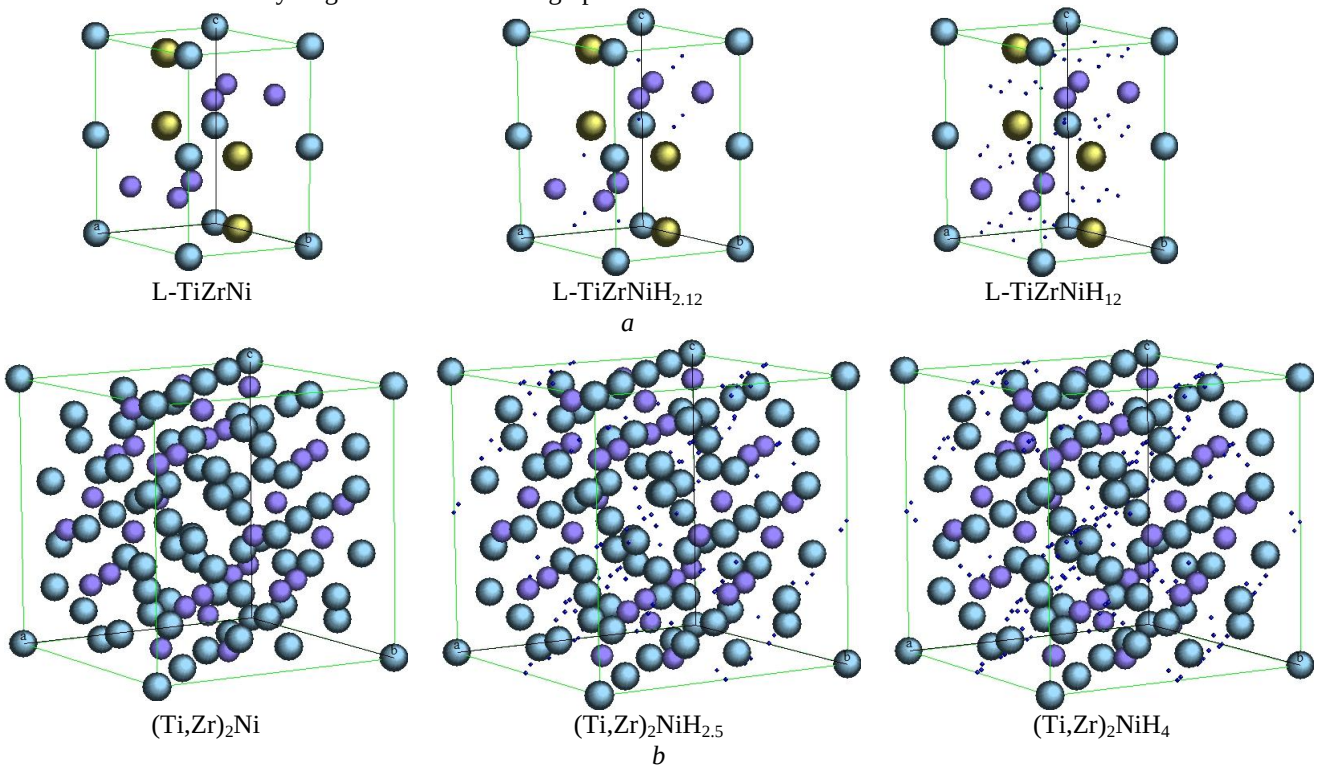

Fig. 4. Crystal structure models of L-TiZrNiH$_x$ (a) and (Ti, Zr)$_2$NiH$_x$ (b) phases with different hydrogen content (● – Ti; ● – Zr; ● – Ni)

The same way analysis of the $(Ti, Zr)_2NiH_{2.5}$ crystal structure shows, that its unit cell consists of 176 atoms (96 metallic atoms and 80 hydrogen atoms). In the case of 100% hydrogen site occupancy it is theoretically possible to obtain the structure $(Ti, Zr)_2NiH_4$ with H:M ratio 4:3 (hydrogen storage 1.98 wt.%). Such theoretical structure should consist of 224 atoms, 128 of which are hydrogen. Crystal structure models of the $(Ti, Zr)_2NiH_x$ phase with different hydrogen content are shown in Fig. 4,b.

In the L-$TiZrNiH_x$ Laves phase hydrogen atoms occupy primarily polyhedral voids between titanium and zirconium atoms (Zr_2Ti_2 polyhedron). This is due to the fact that zirconium and titanium atoms have a larger radius, 2.16 and 2.0 Å, respectively, in comparison with nickel atomic radius 1.62 Å. Therefore, the voids between them are the largest, as it seen in Fig. 5, where the structure models of L-$TiZrNiH_{12}$ and $(Ti, Zr)_2NiH_4$ phases are shown. After the occupying of the polyhedral Zr_2Ti_2 voids hydrogen is located in polyhedral Zr_2TiNi voids. This polyhedron is slightly smaller than the previous one, since one titanium atom is replaced in it by nickel. In the last place hydrogen occupies positions in the Zr_2Ni_2 polyhedral voids. Here, the atoms are located most densely, so hydrogen is the most difficult to occupy the corresponding position.

The situation with the $(Ti, Zr)_2NiH_4$ phase differs crucially from the L-$TiZrNiH_{12}$. As can be seen on Fig. 5,b, in the $(Ti, Zr)_2NiH_4$ phase hydrogen is located primarily in the large octahedral $(Zr, Ti)_6$ voids, and then in smaller tetrahedral Ni_4 voids. Considering the small number of possible voids with a much larger unit cell size (96 metallic atoms in $(Ti, Zr)_2Ni$ and 12 in L-TiZrNi; $V = 1690.69$ Å^3 and $V = 202.78$ Å^3, respectively), it is obvious, that $(Ti,Zr)_2Ni$ phase has a lower hydrogen storage potential. And in the case of $Ti_{30}Zr_{45}Ni_{25}$ melt-spun alloy, it is undesirable, as it reduces the total hydrogen storage capability of the samples.

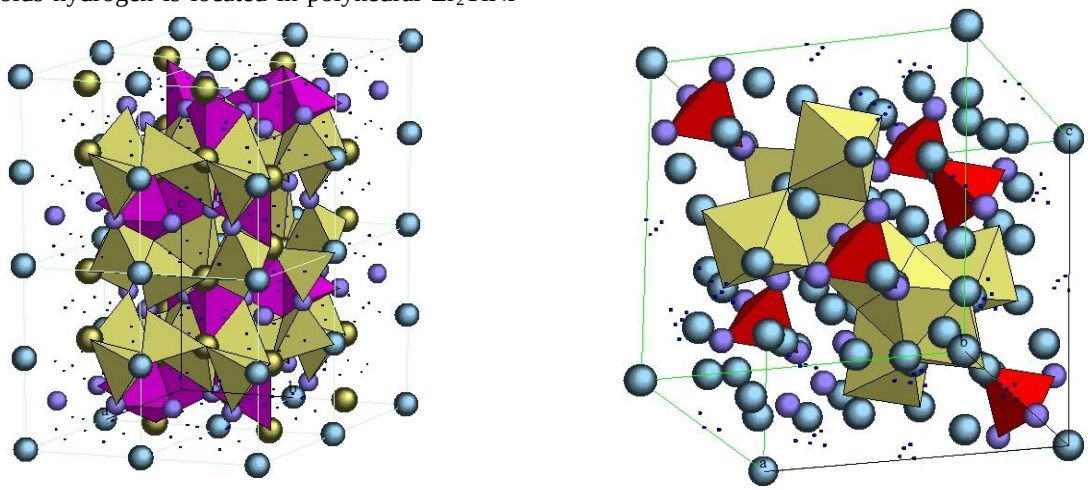

a *b*

Fig. 5. Polyhedral models of L-$TiZrNiH_{12}$ (a) and $(Ti,Zr)_2NiH_4$ (b) phases

Additionally, special attention should be paid to the O_2 control in as-cast and melt-spun alloys and contamination during hydrogen absorption process due to oxygen ability to decrease the hydrogen storage capacity. Firstly, the presence of oxygen destabilizes the i-phase and the Laves phase. Secondly, the presence of oxygen in the alloy leads to the formation of an oxygen-containing phase $(Ti, Zr)_4Ni_2O$, which is practically not involved in the hydrogen accumulation process. The structural model of the $(Ti, Zr)_4Ni_2O$ phase [14] is shown in Fig. 6.

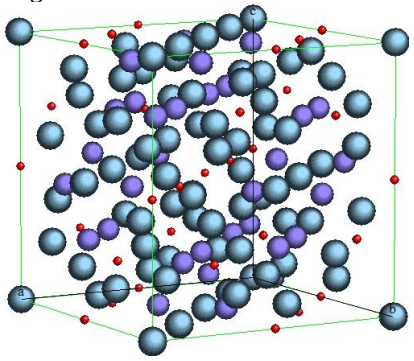

Fig. 6. Crystal structure model of $(Ti, Zr)_4Ni_2O$ phase

Tabl. 2 and Fig.7 shows the results of EDX analysis of as-cast and melt-spun samples. An analysis of these data shows that all the samples correspond to a given value of $Ti_{30}Zr_{45}Ni_{25}$ for titanium, zirconium and nickel, but they have a significant amount of interstitial impurities as oxygen, nitrogen, and carbon. Moreover, the content for oxygen and nitrogen are inversely proportional to the dependence: the amount of oxygen was maximal in the melt-spun samples and decreased with increasing hydrogen temperature, and vice versa, the amount of nitrogen is minimal in the melt-spun samples and increases with increasing hydrogen temperature.

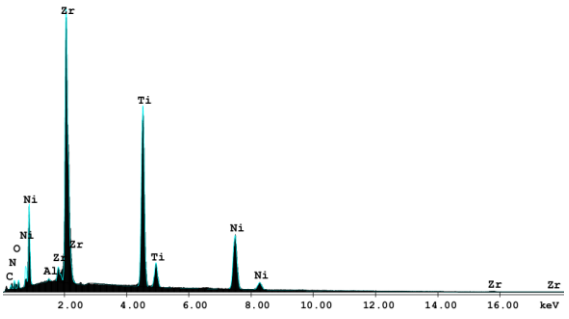

Fig. 7. EDX spectrum of melt-spun $Ti_{30}Zr_{45}Ni_{25}$ alloy

Table 2

The composition of the investigated samples

Element	melt-spun	*T*=400 °C	*T*=450 °C	*T*=500 °C
Ti	27.91	27.8	28.09	27.77
Zr	42.52	42.23	42.14	42.48
Ni	23.51	23.18	23.66	23.75
O	2.29	1.35	1.73	0.48
N	2.41	3.16	3.02	3.71

It should be noted that the oxygen and nitrogen content obtained by EDX analyses differs significantly from the data obtained with the LECO TC-600 gas analyzer. The results of the LECO TC-600 gas analyzer for the nitrogen and oxygen are shown in Fig. 8.

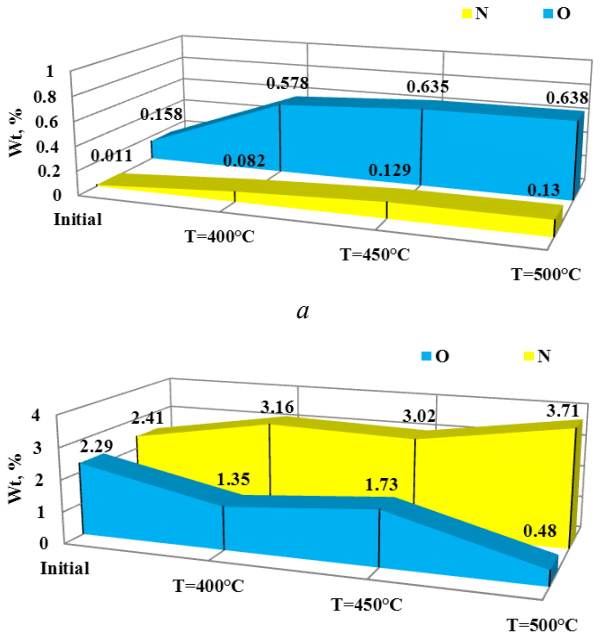

a

b

Fig. 8. Nitrogen and Oxigen content in the $Ti_{30}Zr_{45}Ni_{25}$ alloys: a – LECO, b – QUANTA 200 3D

This discrepancy can be explained by methodological differences. The principle of the gas analyzer is to measure the gas content when the sample is completely melted in a graphite crucible, thus, the obtained data show the volume content of oxygen and nitrogen in the sample. With EDX analysis on a scanning electron microscope, the obtained data show the elemental composition in a thin near-surface layer (1…2 μm). Given the high adsorption capacity of this composition to such gases as O_2 and N_2, the surface of the samples is contaminated while they are in the air between saturation with hydrogen and measurement.

The graph in Fig.8,a shows that an increase in the amount of oxygen and nitrogen is observed in the process of hydrogenation, due to contamination of samples from the gas phase. This is due to the presence of impurities of O_2 and N_2 in hydrogen. The inverse proportional dependence of the amount of oxygen and nitrogen in the test samples, obtained from EDX data, indicates that during hydrogenation, some of the oxygen from the surface is reduced to H_2O and the surface is cleaned.

And the more intense, the higher the saturation temperature. While nitrogen still accumulates more actively in the near-surface layer, as the saturation temperature increases. In addition, comparing the results of both studies, it can be concluded that during the saturation of H_2 from the gas phase at temperatures of 400…500 °C, some oxygen and nitrogen pass from the surface into the sample volume.

SEM analyses (Fig. 9) showed that the structure of the samples did not undergo significant changes in the hydrogenation process in this temperature range. Hydrogen dissolves in the crystal lattice of the sample without forming local clusters in the bulk of material and along the grain boundaries, which also confirmed by XRD analysis.

To eliminate the contamination of samples with oxygen and nitrogen during hydrogenation, $Ti_{30}Zr_{45}Ni_{25}$ alloy was annealed in the pure hydrogen atrmosphere obtained by thermal decomposition of titanium hydride at temperatures above 500 °C with preliminary vacuum pumping, which aimed at removing other gas components. XRD pattern of the sample after hydrogenation in the pure hydrogen is shown in Fig. 10. As can be seen, the annealing in pure hydrogen lead to the formation of two hydrides, based on L-TiZrNi Laves phase (C14) and α-(Ti,Zr) solid solution. The main phase in this sample is L-$TiZrNiH_{2.12}$ (weight fraction – 92.4 wt.%; lattice parameters: a = 5.4273 Å; c = 8.8969 Å; V = 226.96 Å^3; ΔV = 25.2; $\Delta V/V$ = 12.5%). In addition to the Laves phase hydride, the α-(Ti, Zr) phase is also present in the sample in an amount of 7.6 wt.%. The lattice parameters are: a = 3.03 Å; c = 4.82 Å, V = 38.3 Å^3; ΔV = 0.4; $\Delta V/V$ = 1.1%. Giving the small change in the volume of the unit cell for α-(Ti, Zr), one can say that this phase practically did not participate in the hydrogenation process.

It was observed that the sample did not undergo formation of the $(Ti, Zr)_2NiH_x$ or $(Ti, Zr)_4Ni_2O$ phases during the hydrogenation process in the pure hydrogen atmosphere. It is known that latter phase has a detrimental effect on the absorption capacity of the material. Thus, the absence of oxygen impurities in the hydrogen atmosphere is an important factor in increasing the absorption capacity of this system and a necessary condition for achieving theoretically possible 5.73 wt.% H_2 in L-$TiZrNiH_{12}$ (in the case of theoretically 100% filling possible positions with hydrogen).

In addition, it is necessary to lower the hydrogenation temperature, as according to the X-ray data, the maximum amount of hydrogen was absorbed under T = 400 ºC.

SUMMARY

The influence of hydrogen absorption temperature on the structure-phase composition of melt-spun $Ti_{30}Zr_{45}Ni_{25}$ samples subjected to heat treatment in a hydrogen atmosphere at different temperatures (400, 450, 500 °C) for 4 hours was studied.

XRD analysis revealed that hydrides based on the Laves phase L-TiZrNi, $(Ti, Zr)_2Ni$ and α-(Ti, Zr) are formed during the hydrogenation process.

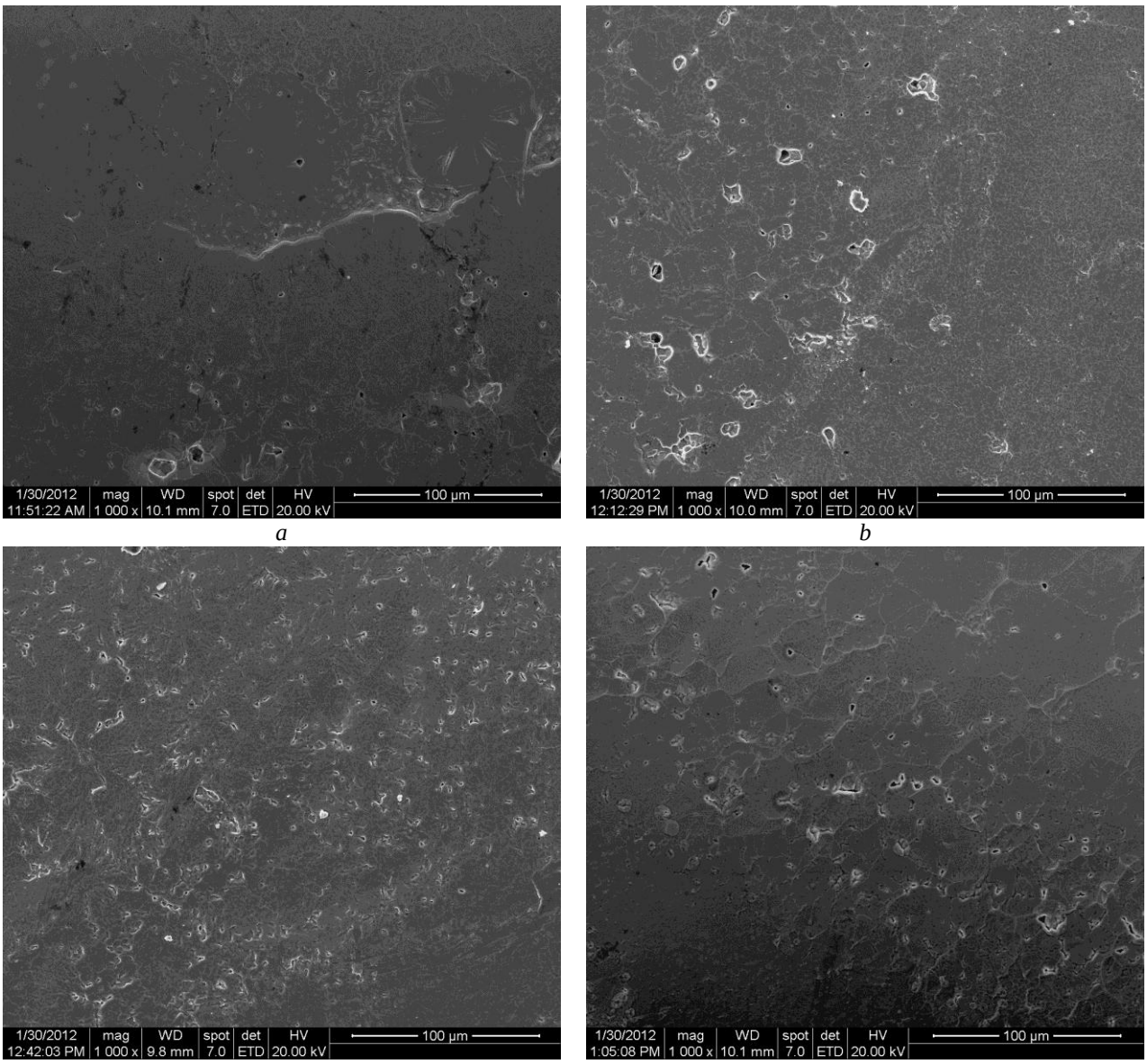

Fig. 9. SEM of melt-spun $Ti_{30}Zr_{45}Ni_{25}$ samples before and after hydrogenation: a – melt-spun sample; b – hydrogenation at T = 400 °C; c – T = 450 °C; d – T = 500 °C

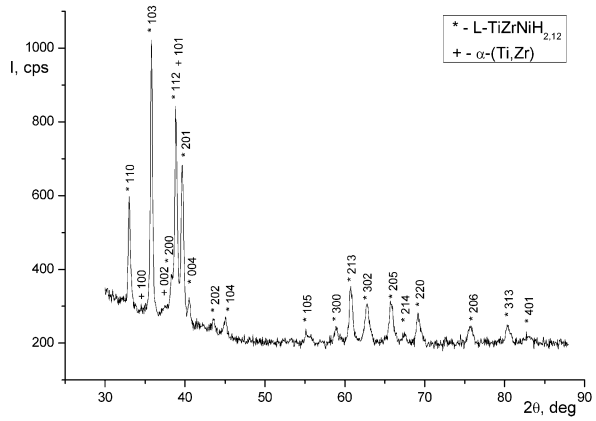

Fig. 10. Diffraction pattern of melt-spun $Ti_{30}Zr_{45}Ni_{25}$ alloy, heat-treated in the pure hydrogen atmosphere

The main phase controlling the structure of the samples and the hydrogen absorption is the L-TiZrNi Laves phase. It was shown that the L-TiZrNi phase at 400 °C absorbs the maximum amount of hydrogen.

Structural models of the phases present in the investigated samples were constructed and a model for filling these phases with hydrogen was presented. It was shown that at a 100% filling of theoretically possible positions, it was expected to obtain a structure of L-TiZrNiH_{12} with the H:M ratio of 4:1 (5.73 wt.% hydrogen storage).

SEM/EDX study of the surface of the samples was carried out and it was shown that the surface of the samples did not undergo significant changes during the hydrogenation.

The influence of the hydrogenation temperature on the concentration of oxygen and nitrogen gas impurities was established.

ACKNOWLEDGEMENTS

Authors thank gratefully to O.M. Bovda for the sample fabrication and R.V. Azhazha for oxygen and nitrogen content measurements. Also, special thanks to M.A. Tikhonovsky and M.M. Pylypenko for the help in discussing the results.

REFERENCES

1. R.M. Azhazha, Yu.P. Bobrov, O.M. Bovda, O.E. Dmytrenko, L.V. Onishenko. Research of processes of sorption-desorption of hydrogen from the rapidly quenched alloys of the Ti-Zr-Ni system // *Problems of Atomic Science and Technology. Series "Vacuum, Pure Materials, Superconductors" (17).* 2008, N 1, p. 129-132.

2. R.M. Stroud, A.M. Viano, E.H. Majzoub, P.C. Gibbons, and K.F. Kelton. Ti-Zr-Ni quazicristals: structure and hydrogen storage // *Mat. Res. Soc. Symp. Proc.* 1996, v. 400, p. 255-260.

3. A.M. Viano, E.H. Maizoub, R.M. Stroud, M.J. Kramer, S.T. Misture, P.C. Gibbons, K.F. Kelton. Hydrogen absorption and storage in quasicrystalline and related Ti-Zr-Ni alloys // *Philosophical Magazine A.* 1998, v. 78, p. 131-141.

4. A. Kocjan, S. Kovacic, A. Gradisek, J. Kovac, P.J. McGuiness, T. Apih, J. Dolinsek, S. Kobe. Selective hydrogenation of Ti-Zr-Ni alloys // *International Journal of Hydrogen Energy.* 2011, v. 36, p. 3056-3061.

5. Yu.P. Bobrov, O.M. Bovda, S.S. Grankin, O.E. Dmytrenko, L.V. Onishenko, O.S. Tortika. Hydrogen absorpting-desorpting behavior of melt-spun Ti30Zr45Ni25 alloy // *Metal Physics and Newest Technologies*. 2008, v. 30, p. 329-336.

6. E. Tuscher. Wasserstoffaufnahme und magnetisches Verhalten der intermetallischen Phasen Ti_2(Ni, Co) und Ti_2(Ni, Fe) // *Monatsh. Chem.* 1980, v. 111, p. 535-546.

7. S.A. Semiletov, R.V. Baranova, Yu.P. Khodyrev, R.M. Imamov, S.I. Zheludeva. // *6 European Crystallogr. Meeting.* Barcelona, Spain, 1980, Abstr. p. 244.

8. I. Levin, V. Krayzman, C. Chiu, K.-W. Moon, L.A. Bendersky. Local metal and deuterium ordering in the deuterated ZrTiNi C14 Laves phase // *Acta Materialia.* 2012, v. 60, p. 645-656.

9. V.M. Azhazha, Yu.P. Bobrov, O.M. Bovda, V.O. Bovda, O.E. Dmytrenko, S.D. Lavrinenko, L.V. Onishchenko, A.S. Tortika. Study gassing when heated in a vacuum hydrogenated alloy Nd-Fe-B // *Problems of Atomic Science and Technology. Series "Vacuum, Pure Materials, Superconductors" (15).* 2006, N 1, p. 156-159.

10. E.H. Majzoubyz, R.G. Hennig, and K.F. Kelton. Rietveld refinement and ab initio calculations of a C14-like Laves phase in Ti-Zr-Ni // *Philosophical Magazine Letters.* 2003, v. 83, N 1, p. 65-71.

11. G.A. Yurko, J.W. Barton, and J. Gordon Parr. The Crystal Structure of Ti_2Ni // *Acta Cryst.* 1959, v. 12, p. 909-911.

12. M.H. Mintz, Z. Hadari, M.P. Dariel // *J. Less-Common Metals*. 1979, v. 63, p. 181-191.

13. R.M. Stroud et al. High temperature x-ray and calorimetric studies of phase transformations in quasicrystalline Ti-Zr-Ni alloys // *J. Mater. Res.* 1997, v. 12, N 2, p. 434-438.

14. I. Zavaliy, G. Wojcik, G. Mlynarek, I. Saldan, V. Yartys, M. Kopczyk. Phase-structural characteristics of $(Ti_{1-x}Zr_x)_4Ni_2O_{0.3}$ alloys and their hydrogen gas and electrochemical absorption–desorption properties // *Journal of Alloys and Compounds.* 2001, v. 314, p. 124-131.

Article received 06.12.2017

ВЛИЯНИЕ ТЕМПЕРАТУРЫ НАСЫЩЕНИЯ ВОДОРОДОМ НА СТРУКТУРУ БЫСТРОЗАКАЛЕННОГО СПЛАВА $Ti_{30}Zr_{45}Ni_{25}$

А.Е. Дмитренко, И.В. Колодий

Проведено исследование влияния температуры насыщения водородом на структурно-фазовый состав образцов быстрозакаленного сплава $Ti_{30}Zr_{45}Ni_{25}$, подвергнутых термообработке в атмосфере водорода, при различных температурах (400, 450, 500 °С) в течение 4 ч. Методом рентгеноструктурного анализа установлено, что в процессе наводороживания образуются гидриды на основе фазы Лавеса L-TiZrNi (C14), фазы $(Ti, Zr)_2Ni$ и α-(Ti, Zr). Построены структурные модели фаз, присутствующих в исследуемых образцах, и представлена модель заполнения этих фаз водородом. Проведено электронно-микроскопическое исследование поверхности образцов и показано, что поверхность образцов не претерпевает существенных изменений в процессе насыщения водородом. Установлено влияние температуры наводороживания на концентрацию газовых примесей кислорода и азота.

ВПЛИВ ТЕМПЕРАТУРИ НАСИЧЕННЯ ВОДНЕМ НА СТРУКТУРУ ШВИДКОЗАГАРТОВАНОГО СПЛАВУ $Ti_{30}Zr_{45}Ni_{25}$

О.Є. Дмитренко, І.В. Колодій

Проведено дослідження впливу температури насичення воднем на структурно-фазовий склад зразків швидкозагартованого сплаву $Ti_{30}Zr_{45}Ni_{25}$ після термообробки в атмосфері водню при різних температурах (400, 450, 500 °С) протягом 4 год. Методом рентгеноструктурного аналізу встановлено, що в процесі насичення воднем утворюються гідриди на основі фази Лавеса L-TiZrNi (C14), фази $(Ti,Zr)_2Ni$ та α-(Ti, Zr). Побудовано структурні моделі фаз, присутніх у досліджуваних зразках, і представлена модель заповнення цих фаз воднем. Проведено електронно-мікроскопічне дослідження поверхні зразків і показано, що поверхня зразків не зазнає істотних змін у процесі насичення воднем. Встановлено вплив температури насичення воднем на концентрацію газових домішок кисню та азоту.